Research Article | Vol. 30, No. 7 / 28 Mar 2022 / Optics Express 11472
Optics EXPRESS

Conversion efficiency improvement of terahertz wave generation laterally emitted by a ridge-type periodically poled lithium niobate

JUNICHI HAMAZAKI,* YOH OGAWA, TADASHI KISHIMOTO, SHIN'ICHRO HAYASHI, NORIHIKO SEKINE, AND IWAO HOSAKO

[1]National Institute of Information and Communications Technology, Tokyo, Japan
[2]Oki Electric Industry Co., Ltd., Saitama, Japan
*hamazaki@nict.go.jp

Abstract: We demonstrate terahertz (THz) wave generation by wavelength conversion in a ridge-type/bulk periodically poled lithium niobate (RT-/bulk-PPLN) under almost the same experimental conditions. When using the RT-PPLN, the ridge structure works as a slab waveguide for the incident pump beam (wavelength: ~1 μm), and the generated THz wave (~200 μm) was emitted uniformly from the entire side surface of the crystal. The RT-PPLN has a much higher conversion efficiency from the pumping beam to the THz wave than the bulk-PPLN, and the ratio improved several ten times compared with those of previous studies.

1. Introduction

Periodically-poled lithium niobates (PPLNs) have attracted much attention as a candidate crystal to generate THz wave, since PPLNs are useful for THz wave generation by the following reasons: (i) large non-linear coefficient d_{eff}~170 pm/V [1,2], (ii) controllability of THz frequency and emission direction by design parameters such as period of PPLN, (iii) high optical damage threshold (MgO-doped LN ~ 0.6 GW/cm^2 for long pulse (~20 ns pulse), 100-120 mJ/cm^2 (peak optical intensity ~ 360 GW/cm^2) for femtosecond pulse (~330 fs pulse)) [3–6], (iv) robust over surrounding environments such as humidity and temperature compared with organic crystals. Therefore, it has been used as an emitter in various THz wave generation experiments not only in cases of femtosecond pulse pumping via optical rectification effect (OR) [7–13] but also quasi-CW (long pulse) pumping via different frequency generation (DFG) [14–18]. Moreover, PPLN has been proposed to be used as a crystal for cascade parametric oscillation for highly efficient THz wave generation [19].

For efficient THz wave emission, lateral THz wave generation in bulk PPLN with slant-stripe periodical structure (bulk-PPLN) have been applied [14, 20–22]. In this case, main advantage is that absorption of THz wave due to the material absorption can be avoided, *e.g.*, ~28 cm^{-1} at 1.5 THz and >170 cm^{-1} at >2.5 THz [23–25]. Moreover, damage threshold of LN for femtosecond pulse is about 3 orders of magnitude higher than that for long pulse, as explained above, lateral THz wave generation from PPLN pumped by femtosecond pulse is suitable to obtain high power output.

For further improvement, a ridge-type PPLN (RT-PPLN) was proposed in Refs. [26,27]. By fabricating the ridge structure of PPLN (width~20 μm, hight~330 μm, length ~ 20 mm), which works as a slab waveguide for pump beam, high-power electric-field density due to the optical confinement with long interaction length is expected. However, the output from RT-PPLN in Ref. [26,27] was about 1/30, compared with bulk-PPLN in Ref. [15]. Here, the pump light sources in these papers were the same. The reason why the output from RT-PPLN was reduced has not been mentioned in Refs. [26,27]. Since waveguide THz sources are expected to be more efficient than a bulk THz wave sources, various waveguide THz sources using LN have been proposed

#450876 https://doi.org/10.1364/OE.450876
Journal © 2022 Received 27 Dec 2021; revised 27 Feb 2022; accepted 4 Mar 2022; published 22 Mar 2022

Optics EXPRESS

recently [28,29]. However, first of all, it is important to confirm that the waveguide structure is effective in THz sources.

In this paper, we experimentally demonstrate that THz wave generation from RT-PPLN is efficient compared with that from bulk-PPLN. Pumping by femtosecond pulse, output power from RT-PPLN was about twice of that from bulk-PPLN. This improvement is explained by the effective utilization of the ridge structure as a slab-waveguide. We confirmed that the ridge structure works as nearly ideal slab waveguide, and THz waves are generated from the whole side surface of the ridge. Moreover, we investigated effect of incident NA of pump beam to THz wave intensity, to clarify optimal focusing condition of the pump beam into the ridge structure.

2. Experimental setup

Figure 1(a) shows microscope image of RT-PPLN from the front. The ridge structure (width of ~20 μm, height of ~330 μm, and length of ~42 mm) was fabricated by a dicing saw from 500 μm-thick PPLN substrate, which works as a slab waveguide for optical pump. Its pitch length is ~91 μm and its direction is parallel to the longitudinal direction of the ridge, as shown in Fig. 1(b). By this periodical structure, THz wave at 1.5 THz generates in the lateral direction of the ridge, which is almost the same structure in Ref. [27]. Note that, the structure does not satisfy the phase matching condition. However, it is relaxed in this case. This is because the width of the ridge is shorter than the wavelength of the terahertz wave, as mentioned in Ref. [27].

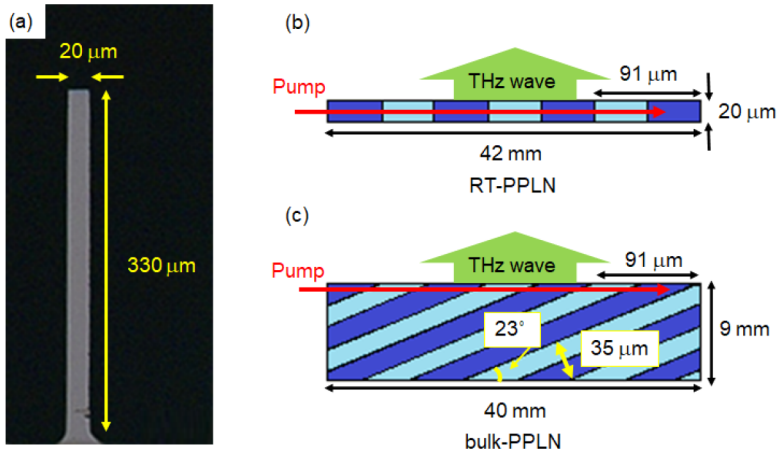

Fig. 1. (a)Microscope image of RT-PPLN from the front. Schematic structures of RT-PPLN (b) and bulk-PPLN (c).

For comparison, we also fabricated bulk-PPLN (thickness of ~ 500 um, length of ~40 mm). Its pitch length is ~35 μm with angle of ~23 degree, as shown in Fig. 1(c). This periodical structure is designed to generate THz-wave at 1.5 THz in the lateral direction, which is the same as the structure in Ref. [14].

About the effect of material absorption of generated THz wave, it is estimated to be ~5% and ~20% at the maximum for RT- and bulk-PPLN, respectively, (considering absorbance to be ~28 cm^{-1} and each horizontal beam sizes). Especially, THz wave absorption in RT-PPLN is avoided enough due to its thin ridge width to be ~20 μm, Thus, it is not necessary to reduce LN absorbance by cooling [8].

Figure 2 shows our experimental setup. Femtosecond pump pulses (duration time ~ 120 fs, center wavelength = 1035 nm, full width at half maximum (FWHM) ~20 nm, average power >1.8 W, and repetition rate ~30 MHz) were focused onto the RT-PPLN by two cylindrical lenses (CL_1 and CL_2). CL_1 and CL_2 have focal lengths of 250 mm and 25.4 mm in vertical and horizontal

Optics EXPRESS

directions, respectively. Polarization angle of the pump beam was set in vertical direction, which was parallel to the polarization direction of the RT-PPLN. In the vertical direction, the pump beam was focused slowly into RT-PPLN and its focal point was adjusted around the center of the ridge with a beam size of ~75 μm, to generate THz wave from the whole side-surface of the ridge. In the horizontal direction, the pump beam was confined by the ridge with its width of ~ 20 μm.

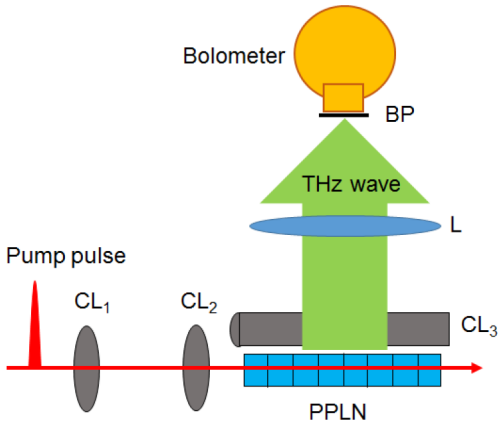

Fig. 2. Experimental setup. CL: Cylindrical lens, L: Plano-convex lens, BP: Black polyethylene.

Transmittance of the RT-PPLN was measured to be ~65%. Considering twice Fresnel reflection on the surfaces of ~14% (refractive index of LN ~ 2.2), coupling efficiency of the pump beam was evaluated to be 90%. Moreover, depletion of the pump beam by THz wave generation was not observed in our experiments.

Generated lateral THz wave from the side-surface was collected by aspheric cylindrical THz lens (CL_3) with sizes of height 30 mm, length 60 mm, and an effective focal length 9 mm. After that, the THz wave was focused into the cryogenic bolometer by THz lens (L) with focal length of 100 mm and its diameter of 76 mm. The THz wave signal was detected by lock-in detection technique. Black polyethylene (BP) was used to block scattering light and prevent background noise.

In the case of the bulk-PPLN, experimental setup was as same as the case of RT-PPLN, but the pump beam was focused by convex lens with $f = 250$ mm, in place of the CL_1 and CL_2 in Fig. 2. In this case, focus spot was circular, and its diameter was estimated to be ~75 μm.

From RT- and bulk-PPLN, the anticipated electric field profile of the generated THz wave in the lateral direction is multicycle THz wave pulse [21]. At the same time, multi-cycle THz wave pulse in collinearly with the pump beam is also produced at different frequency (~1.1 THz). However, this THz wave is mostly absorbed due to the material absorption of LN [23–25]. Note that, in this experiment, we measured simple THz wave radiation from both RT- and bulk-PPLN, not THz wave emission as Cherenkov waves. To obtain such THz wave, coupling prism to permit the generated THz wave to coupled out into free space is necessary [28].

3. Result

Figure 3 shows average THz-wave powers from RT-PPLN (red circle) and bulk-PPLN (black square) as a function of the average pump power. Both signals increased proportional to the square of the pump power increased. Maximum average power of THz wave from RT- and bulk-PPLN were estimated to be ~7.4 and ~3.6 nW, respectively, at 1.8 W pumping. Moreover, for RT-PPLN, THz wave output was observed to be almost constant over the PPLN length direction. THz waves generation from the whole side surface uniformly were confirmed.

Optics EXPRESS

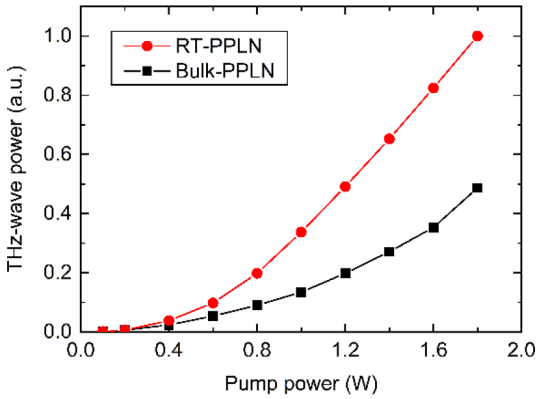

Fig. 3. Average THz-wave powers from RT-PPLN (red circle) and bulk-PPLN (black square) as a function of the average pump power.

Figure 4 shows the output signals from RT-PPLN depended on the pump incident NA. In cases of NA = 0.08, 0.04, 0.02, and 0.01, cylindrical lens with f = 12.7, 25.4, 50, and 100 mm were used respectively, instead of the CL_2 in Fig. 2. As discussed later, the incident pump beam couples into the ridge waveguide regardless of NA. In all the cases, the transmittance of the incident pump beam was almost constant to be ~65%.

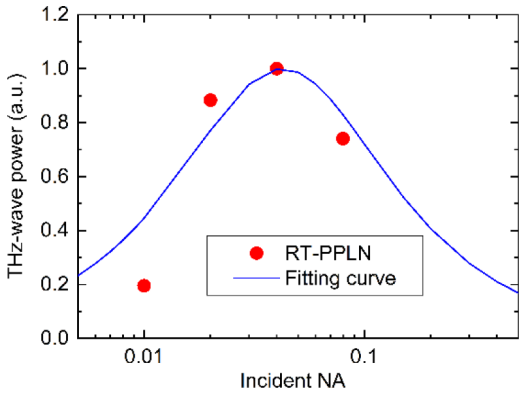

Fig. 4. Average output power of the THz wave output from RT-PPLN at 1.8 W pumping power, as a function of the incident NA. Blue line denotes fitting curve calculated from the coupling efficiency of incident beam and fundamental waveguide mode, obtained by the equation $\eta = 2a/(1 + a^2)$, where $a = \mathrm{NA_{incident}}/\mathrm{NA_{ridge}}$. $\mathrm{NA_{incident}}$ and $\mathrm{NA_{ridge}}$ denote the NA of incident beam and NA of fundamental mode in the ridge, respectively. Result was best fitted when $\mathrm{NA_{ridge}} \approx 0.043$.

Maximum output was obtained when the incident NA = 0.04. The output power decreased as the NA differed from 0.04. The blue line in Fig. 3 denotes the fitting curve calculated by coupling efficiency of incident beam and fundamental waveguide mode, given by $\eta=2a/(1 + a^2)$, where $a = \mathrm{NA_{incident}}/\mathrm{NA_{ridge}}$ [30]. The calculated line was well fitted the experimental result when $\mathrm{NA_{ridge}}$ ~0.043.

Optics EXPRESS

4. Discussion

In our experiments, THz wave powers from RT-PPLN was about twice higher than that from bulk-PPLN. However, a simple theoretical calculation indicates that the ratio of THz wave powers from RT-PPLN to that from bulk-PPLN is ~6, as discussed below.

Since THz wave is generated via second-order nonlinear optical process, output power of THz wave (P_{THz}) is proportional to the square of pumping intensity (P_{pump}/S, where P_{pump} and S denote pumping power and spot area of the pump beam, respectively), proportional to the linear of interaction volume (LS, where L denotes interaction length), P_{THz} is approximately given as follows [31–33].

$$P_{THz} = A\frac{L}{S}|P_{Pump}|^2 \tag{1}$$

where A is the coefficient for generating THz wave from PPLN. In our cases, material absorption is negligible, as pump spot size is less than penetration depth of THz wave to be ~300 μm at 1.5 THz, which was evaluated by absorbance ~ 28 cm^{-1} at 1.5 THz in Ref. [24].

According to E.q. (1), THz wave generation efficiency is proportional to L_{eff}/S_0 when the pump power is the same. Here, L_{eff} is defined as twice the length from the focal point where is half of the excitation density of the spot. Generally, in cases of waveguides, smaller beam spot area and longer interaction length are expected due to optical confinement by waveguide structure, compared with cases of bulk.

In the case of RT-PPLN, S and L_{eff} are estimated to be ~1500 μm^2 (vertical ~75 μm, horizontal ~20 μm) and ~20 mm, respectively. On the other hand, in the case of bulk-PPLN, S and L_{eff} are estimated to be ~4400 μm^2 (focal diameter ~75 μm) and ~10 mm, respectively. The difference in L_{eff} between RT-PPLN and bulk-PPLN is due to the beam divergence angle extends to one and two dimensions, respectively. Substituting these values into L_{eff}/S, it is evaluated that ratio of output from RT-PPLN to that from bulk-PPLN is about 6. This ratio is higher than the ratio obtained from our experiments to be ~2.2, which was evaluated by performing the quadratic approximation of the graphs in Fig. 3.

Next, we discuss what causes the difference between the experimental result and numerical evaluation. Considering the ridge structure with a width of 20 μm, it works as a multimode slab waveguide. Its V-parameter is evaluated about 80, assuming refractive index of core and clad are 2.2 and 1, respectively [34]. Therefore, it contains several ten modes, not as single mode. Thus, the pump beam incident on the ridge is affected by the modal dispersion by the ridge structure. Although the transmittances of the pump beams were almost constant, the output of the THz wave decreased as the mismatch between the incident NA and the ridge NA (~0.04) increased, as shown in Fig. 3. This indicates that mode matching of pump beam into the fundamental mode in the ridge is contributed to generate THz waves efficiently.

About the comparative investigation of lateral THz wave generation from RT- and bulk-PPLN, to the best of our knowledge, this paper demonstrated that RT-PPLN generates THz waves more efficiently than bulk-PPLN for the first. The works in Refs. [27] and [15], output of lateral THz wave generation via DFG from RT-PPLN and bulk-PPLN were reported, respectively, pumped by the same pump source. Comparing these papers, the output power from RT-PPLN was about 1/30 of that from bulk-PPLN. The reason is explained as follows.

In the experiment in Ref. [27], the incident beam was focused into ridge structure by a $r = 1$ mm rod lens together with $f = 100$ mm circular lens. Owing to a high NA focused by the rod lens (NA~0.5 in typical), large mode mismatching of the incident pump beam to fundamental waveguide mode in the ridge was considered. Moreover, a large aberration due to the rod lens was also considered. Owing to these reasons, THz wave was not efficiently generated from the ridge.

Finally, for further improvement, it is desirable to have a narrower ridge width, *i.e.*, single mode ridge. By doing that, only the fundamental mode is excited in RT-PPLN and its excitation

Optics EXPRESS

density becomes further high. When ridge width is ~1 μm, efficiency of THz wave generation from RT-PPLN will be improved more than 100 times compared to that from bulk PPLN.

5. Summary

In this paper, we demonstrated that THz wave generation from RT-PPLN was more efficient than that from bulk PPLN, by comparing outputs from RT- and bulk-PPLN under almost the same experimental conditions. As the ridge structure of RT-PPLN works as an almost ideal slab waveguide for incident pump beam, electric-field density was high power due to the optical confinement with long interaction length. Moreover, it was confirmed that THz waves were generated uniformly from the whole side-surface of the ridge. The ratio of THz wave output from RT-PPLN to that from bulk-PPLN was improved from ~1/30 (by comparing the Refs. [27] and [15]) to be ~2.2. This improvement was obtained by optimizing the incident condition of the pump beam.

To obtain efficient THz wave generation, it is important to couple pump beams into fundamental mode of ridge structures, which was clarified by investigating the output of THz wave depended on incident NA. Moreover, we mentioned that the efficiency of THz wave generation will be significantly improved by using a single-mode RT-PPLN with thin ridge width to be ~1 μm.

Acknowledgment. We thank Prof. Takashige Omatsu, and Associate Prof. Katsuhiko Miyamoto (Chiba univ.) for useful discussion and helpful comments on our experiments.

Disclosures. The authors declare no conflicts of interest.

Data availability. Data underlying the results presented in this paper are not publicly available at this time but may be obtained from the authors upon reasonable request.

References

1. J. Hebling, K.-L Yeh, M.C. Hoffmann, B. Bartal, and K. A. Nelson, "Generation of high-power terahertz pulses by tilted-pulse-front excitation and their application possibilities," J. Opt. Soc. Am. B **25**(7), B6–B19 (2008).
2. A. Yuriv, *Quantum Electronics* (Wiley, 1989).
3. J. L. Nightingale, W. J. Silva, G. E. Reade, A. Rybicki, W. J. Kozlovsky, and R. L. Byer, "Fifty percent conversion efficiency second harmonic generation in magnesium doped lithium niobite," Proc. SPIE 0681, Laser and Nonlinear Optical Materials, (9 March 1987).
4. J. Y. Yao, "Wang Nonlinear Optics and Solid-State Lasers: Advanced Concepts," Tuning-Fundamentals and Applications, Springer2012).
5. D.N. Nikogosyan, "Nonlinear Optical Crystals: A Complete Survey," (Springer, 2006).
6. F. Bach, M. Mero, M.-H. Chou, and V. Petrov, "Laser induced damage studies of $LiNbO_3$ using 1030-nm, ultrashort pulses at 10-1000 kHz," Opt. Mat. Express **7**(1), 240–252 (2017).
7. Y.-S. Lee, T. Meade, V. Perlin, H. Winful, T. B. Norris, and A. Galvanauskas, "Generation of narrow-band terahertz radiation via optical rectification of femtosecond pulses in periodically poled lithium niobate," Appl. Phys. Lett. **76**(18), 2505–2507 (2000).
8. Y.-S. Lee, T. Meade, T. B. Norris, and A. Galvanauskas, "Tunable narrow-band terahertz generation from periodically poled lithium niobate," Appl. Phys. Lett. **78**(23), 3583–3585 (2001).
9. C. Zhang, Y. Avetisyan, A. Glosser, I. Kawayama, H. Murakami, and M. Tonouchi, "Bandwidth tunable THz wave generation in large-area periodically poled lithium niobate," Opt. Express **20**(8), 8784–8790 (2012).
10. S. Carbajo, J. Schulte, X. Wu, K. Ravi, D. N. Schimpf, and F.X. Kartner, "Efficient narrowband terahertz generation in cryogenically cooled periodically poled lithium niobate," Opt. Lett. **40**(24), 5762–5765 (2015).
11. J. Hamazaki, Y. Ogawa, N. Sekine, A. Kasamatsu, A. Kanno, N. Yamamoto, and I. Hosako,"Broadband frequency-chirped terahertz-wave signal generation using periodically-poled lithium niobate for frequency-modulated continuous wave radar application," Proc. SPIE 9747, Terahertz, RF, Millimeter, and Submillimeter-Wave Technology and Applications IX, 97471J (2016).
12. F. Ahr, S. W. Jolly, N. H. Matlis, S. Carbajo, T. Kroh, K. Ravi, D. N. Schimpf, J. Schulte, H. Ishizuki, T. Taira, A. R. Maier, and F. X. Kartner, "Narrowband terahertz generation with chirped-and-delayed laser pulses in periodically poled lithium niobate," Opt. Lett. **42**(11), 2118–2121 (2017).
13. F. Lemery, T. Vinatier, F. Mayet, R. Asmann, E. Baynard, J. Demailly, U. Dorda, B. Lucas, A.-K. Pandey, and M. Pittman, "Highly scalable multicycle THz production with a homemade periodically poled microcrystal," Commun. Phys. **3**(1), 150 (2020).
14. Y. Sasaki, A. Yuri, K. Kawase, and H. Ito, "Terahertz-wave surface-emitted difference frequency generation in slant-stripe-type periodically poled LiNbO3 crystal," Appl. Phys. Lett. **81**(18), 3323–3325 (2002).

Optics EXPRESS

15. Y. Sasaki, Y. Avetisyan, H. Yokoyama, and H. Ito, "Surface-emitted terahertz-wave difference-frequency generation in two-dimensional periodically poled lithium niobate," Opt. Lett. **30**(21), 2927–2929 (2005).
16. T. D. Wang, S. T. Lin, Y. Y. Lin, A.C. Chiang, and Y.C. Huang, "Forward and backward terahertz-wave difference-frequency generations from periodically poled lithium niobate," Opt. Express **16**(9), 6471–6478 (2008).
17. R. Sowade, I. Breunig, I. C. Mayorga, J. Kiessling, C. Tulea, V. Dierolf, and K. Buse, "Continuous-wave optical parametric terahertz source," Opt. Express **17**(25), 22303–22310 (2009).
18. K. Nawata, Y. Tokizane, Y. Takida, and H. Minamide, "Tunable backward terahertz-wave parametric oscillation," Sci. Rep. **9**(1), 726 (2019).
19. K. Ravi, M.l Hemmer, G. Cirmi, F. Reichert, D. N. Schimpf, O. D. Mucke, and F. X. Kartner, "Cascaded parametric amplification for highly efficient terahertz generation," Opt. Lett. **41**(16), 3806–3809 (2016).
20. J. A. Lhuillier, G. Torosyan, M. Theuer, Y. Avetisyan, and R. Beigang, "Generation of THz radiation using bulk, periodically and aperiodically poled lithium niobate – Part 1: Theory," Appl. Phys. **B 86**(2), 185–196 (2007).
21. J. A L'huillier, G. Torosyan, M. Theuer, Y. Avetisyan, and R. Beigang, "Generation of THz radiation using bulk, periodically and aperiodically poled lithium niobate – Part 2: Experiments," Appl. Phys. B **86**(2), 197–208 (2007).
22. C. Weiss, G. Torosyan, J. –P. Meyn, R. Wallenstein, R. Beigang, and Y. Avetisyan, "Tuning characteristics of narrow band THz radiation generated via optical rectification in periodically poled lithium niobate," Opt. Express **8**(9), 497–502 (2001).
23. D. A. Bosomword, "The far infrared optical properties of $LiNbO_3$," Appl. Phys. Lett. **9**(9), 330–331 (1966).
24. X. Wu, C. Zhou, W. R. Huang, F. Ahr, and F. X. Kartner, "Temperature dependent refractive index and absorption coefficient of congruent lithium niobate crystals in the terahertz range," Opt. Express **23**(23), 29729–29737 (2015).
25. L. Palfalvi, J. Hebling, J. Kuhl, A. Peter, and K. Polgar, "Temperature dependence of the absorption and refraction of Mg-doped congruent and stoichiometric $LiNbO_3$ in the THz range," J. Appl. Phys. **97**(12), 123505 (2005).
26. Y. Suzuki, K. Suitsu, Y. Sasaki, I. Ito, and A. Yuri, "Surface emitted THz-wave generation/amplification using ridge-type PPLN," IEICE Tech. Rep. E D2005 (2006).
27. K. Suizu, Y. Suzuki, Y. Sasaki, H. Ito, and Y. Avetisyan, "Surface-emitted terahertz-wave generation by ridged periodically poled lithium niobate and enhancement by mixing of two terahertz waves," Opt. Lett. **31**(7), 957–959 (2006).
28. B. N. Carnio, B. Y. Shahriar, E. Hopmann, and A. Y. Elezzabi, "Excitation mode-dependent terahertz radiation generation from a sub-wavelength Si-SiO_2-$LiNbO_3$-polymer-Si planar waveguide," IEEE Tran. Terahertz. Sci. and Technol. **11**(4), 462–465 (2021).
29. M De Regis, L Consolino, S Bartalini, and P De Natale, "Waveguided approach for difference frequency generation of broadly-tunable continuous-wave terahertz radiation," Appl. Sci. **8**(12), 2374 (2018).
30. K. Kataoka, "Estimation of Coupling Efficiency of Optical Fiber by Far-Field Method," Opt. Rev. **17**(5), 476–480 (2010).
31. T. Tanabe, J. Nishizawa, K. Suto, Y. Watanabe, T. Sasaki, and Y. Oyama, "Terahertz wave generation from GaP with continuous wave and pulse pumping in the 1-1.2 μm region," Mat. Trans. **48**(5), 980–983 (2007).
32. K. L. Vodopyanov, "Optical generation of narrow-band terahertz packets in periodically-inverted electro-optic crystals: conversion efficiency and optimal laser pulse format," Opt. Express **14**(6), 2263–2276 (2006).
33. Y. Avetisyan, Y. Sasaki, and H. Ito, "Analysis of THz-wave surface-emitted difference-frequency generation in periodically polled lithium niobate waveguide," Appl. Phys. B **73**(5-6), 511–514 (2001).
34. Y. Kokubun, *Lightwave Engineering* (CRC, 2018).